

Mixed dispersion nonlinear Schrödinger equation in higher dimensions: theoretical analysis and numerical computations

Atanas Stefanov

*Department of Mathematics, University of Alabama - Birmingham,
1402 10th Avenue South Birmingham AL 35294, USA **

Georgios A. Tsolias

Department of Mathematics and Statistics, University of Massachusetts, Amherst Amherst, MA 01003, USA[†]

Jesús Cuevas-Maraver

*Grupo de Física No Lineal, Departamento de Física Aplicada I,
Universidad de Sevilla. Escuela Politécnica Superior, C/ Virgen de Africa, 7, 41011-Sevilla, Spain
Instituto de Matemáticas de la Universidad de Sevilla (IMUS). Edificio Celestino Mutis. Avda. Reina Mercedes s/n, 41012-Sevilla, Spain[‡]*

Panayotis G. Kevrekidis

Department of Mathematics and Statistics, University of Massachusetts, Amherst Amherst, MA 01003-9305, USA[§]

(Dated: May 6, 2022)

In the present work we provide a characterization of the ground states of a higher-dimensional quadratic-quartic model of the nonlinear Schrödinger class with a combination of a focusing biharmonic operator with either an isotropic or an anisotropic defocusing Laplacian operator (at the linear level) and power-law nonlinearity. Examining principally the prototypical example of dimension $d = 2$, we find that instability arises beyond a certain threshold coefficient of the Laplacian between the cubic and quintic cases, while all solutions are stable for powers below the cubic. Above the quintic, and up to a critical nonlinearity exponent p , there exists a progressively narrowing range of stable frequencies. Finally, above the critical p all solutions are unstable. The picture is rather similar in the anisotropic case, with the difference that even before the cubic case, the numerical computations suggest an interval of unstable frequencies. Our analysis generalizes the relevant observations for arbitrary combinations of Laplacian prefactor b and nonlinearity power p .

I. INTRODUCTION

The nonlinear Schrödinger equation [1–4] is a well-established model characterizing a wide range of physical settings extending from deep water waves [3] to electromagnetic wave evolution in optical fibers [5, 6], and from dilute gases of atomic condensates [4, 7, 8] to waves in plasmas [9, 10]. However, in recent years, biharmonic dispersive-wave models have been gaining considerable traction due to their own emergence in a variety of applications. Arguably, one of the most notable examples thereof is due to the experimental realization of dispersion engineering in laboratory optical systems [11] that enabled quartic dispersion and, through the competition of that with nonlinearity, the formation of the so-called pure-quartic solitons (PQS) [11]. This type of dispersion engineering is also responsible for the realization of the so-called pure-quartic soliton laser [12]. In fact, even pure dispersion of higher orders has been explored, e.g., in [13], giving rise to considerations of conveniently programmable dispersions in fiber lasers [13]. As explained in further detail, e.g., in [11], the prototypical physical system, on account of which such models have recently been intensely explored, involves dispersion-engineered photonic crystal waveguides. In such optical settings, the ability to suitably manipulate dispersion in competition with effects of self-phase modulation is the principal reason for the ability to generate, as well as experimentally observe such solitary waves. Motivated by these developments, numerous mathematical works have explored the existence and stability of solitary waves in such settings [14–16]. The accessibility of a wide range of dispersion profiles has revived considerations of different co-existing types of dispersion, e.g., in the form of a quadratic and a quartic term, as e.g. in the work of [17]. The latter setting has been previously explored, e.g., in the classic works of [18, 19]. Similar competitions between the quadratic and quartic dispersion have also been recently considered in the wave equation setting, giving rise to different bound states and intriguing dynamical phenomena [23].

It is indeed this topic of competing Laplacian and biharmonic terms that we revisit in the present work, especially with a view to higher-dimensional considerations and the interplay of the power (exponent) p of the nonlinearity and the dimen-

* stefanov@uab.edu

† gtsolias@umass.edu

‡ jcuevas@us.es

§ kevrekid@umass.edu

sionality d of the linear operator. More precisely, we shall consider the following mathematical models:

$$i u_t + \Delta^2 u + b \Delta u - |u|^{p-1} u = 0, \quad x \in \mathbf{R}^d \quad (\text{I.1})$$

$$i u_t + \Delta^2 u + b \partial_{x_1}^2 u - |u|^{p-1} u = 0, \quad x \in \mathbf{R}^d \quad (\text{I.2})$$

Our work will be about the study of solitary waves of such models and their stability properties. In fact, we consider standing waves in the form $u = e^{-i\omega t} \Phi$, which results in the elliptic profile equations:

$$\Delta^2 \Phi + b \Delta \Phi + \omega \Phi - |\Phi|^{p-1} \Phi = 0, \quad x \in \mathbf{R}^d \quad (\text{I.3})$$

$$\Delta^2 \Phi + b \partial_{x_1}^2 \Phi + \omega \Phi - |\Phi|^{p-1} \Phi = 0, \quad x \in \mathbf{R}^d \quad (\text{I.4})$$

We will refer to the model (I.1) as the isotropic case, while the model (I.2) as the anisotropic case (due to its different dispersion along the direction x_1). Next, we set up the linear stability framework for these models. Namely, taking $u = e^{-i\omega t} (\Phi + v)$, plugging this in (I.1) (or (I.2) respectively) and ignoring the higher order terms (i.e. super-linear ones of the form $O(v^2)$), we obtain for $\vec{v} = (\Re v, \Im v)$,

$$\vec{v}_t = \mathcal{J} \mathcal{L} \vec{v}, \quad \mathcal{J} = \begin{pmatrix} 0 & -1 \\ 1 & 0 \end{pmatrix}, \quad \mathcal{L} = \begin{pmatrix} \mathcal{L}_+ & 0 \\ 0 & \mathcal{L}_- \end{pmatrix} \quad (\text{I.5})$$

$$\mathcal{L}_+ = \Delta^2 + b \Delta + \omega - p |\Phi|^{p-1}, \quad (\text{I.6})$$

$$\mathcal{L}_- = \Delta^2 + b \Delta + \omega - |\Phi|^{p-1}. \quad (\text{I.7})$$

Similarly, the eigenvalue problem for the anisotropic model (I.2) is also in the form (I.5), with \mathcal{L}_\pm given by

$$\begin{cases} \mathcal{L}_+ = \Delta^2 + b \partial_{x_1}^2 + \omega - p |\Phi|^{p-1}, \\ \mathcal{L}_- = \Delta^2 + b \partial_{x_1}^2 + \omega - |\Phi|^{p-1} \end{cases}$$

We now give a formal definition of spectral stability, which, in the context of the standing waves of the model of interest, is the central focus of the present work.

Definition 1. *We say that the corresponding standing wave solution $e^{-i\omega t} \Phi$ is spectrally stable, provided the eigenvalue problem $\mathcal{J} \mathcal{L} v = \mu v$ does not have non-trivial solution $(v, \mu) : v \in H^4(\mathbf{R}^d), \mu : \Re \mu > 0$.*

The closest in spirit work to the present one is that of [19]. In it, however, the author considers a different model, namely

$$i u_t + \gamma \Delta^2 u + \Delta u + |u|^{p-1} u = 0, \quad x \in \mathbf{R}^d. \quad (\text{I.8})$$

The authors obtains a number of useful (and mostly rigorous) results for the standing waves for these models, especially in the regime¹ $\gamma < 0, |\gamma| \ll 1$. Note however that this case, after some rescaling is equivalent to the case $b < 0$ in (I.1), whereas our main interest is in the case $b > 0$. The latter involves a competition (rather than a cooperation) of the linear contributions and, hence, represents a case of particular interest.

In the present setting, we will examine systematically the isotropic case, but also compare it with the anisotropic one whereby the Laplacian operator is replaced by a second partial derivative along only a single spatial direction. We will present theoretical results in both cases for the ground states of the system and their stability as a function of the nonlinearity power p and the coefficient of the Laplacian (or of the one-dimensional second partial derivative) b . Our principal theorems are, accordingly, stated in the next Section. We note in passing the broad appeal of the topic of spectral stability of solitary waves in a variety of related nonlinear dispersive-wave models, as evidenced, e.g., in the works of [20–22].

We corroborate our theoretical analysis with detailed numerical computations that illustrate systematically both the isotropic and the anisotropic case with $d = 2$, as a function of b and also as a function of p . Starting with the isotropic case, we find that up to the cubic case of $p = 3$, the relevant ground states are generically stable, irrespectively of the value of b . Beyond $p = 3$ and for $3 < p < 5$, a critical threshold of b exists such that below the relevant threshold, the wave is spectrally stable, while above, it destabilizes. Further, above $p = 5$ and below a critical p , the waves will only be spectrally stable for an interval of b 's, while upon crossing this critical threshold, a saddle-center bifurcation leads to the disappearance of all stable solutions of the isotropic setting. Interestingly, the anisotropic example bears numerous similarities with the above described isotropic case. The most notable difference that is worth highlighting is that even below $p = 3$, the anisotropic case may bear instabilities for a narrow interval of b -values; more details will be shown in our numerical computations that follow.

¹ Note that the case $\gamma > 0$ in (I.8) is not as relevant physically as it does not support (bright) localized waves. It basically corresponds to the de-focusing case in the standard NLS framework.

II. MATHEMATICAL SETUP AND MAIN RESULTS

We start by noting that the problem of interest possesses continuous spectrum, which effectively, per Weyl's theorem [24], amounts to the spectrum of the homogeneous background state: $\sigma(\mathcal{L}_\pm) = \sigma(\Delta^2 + b\Delta) = \text{Range}[\xi \rightarrow |\xi|^4 - b|\xi|^2 + \omega] = [\omega - \frac{b^2}{4}, +\infty)$. If we do not expect embedded eigenvalues in the essential spectrum², and since by a direct inspection $\mathcal{L}_-[\Phi] = 0$, so $0 \in \sigma_{p.p.}(\mathcal{L}_-)$ (where $\sigma_{p.p.}$ denotes the pure point spectrum), then we can clearly conclude $\omega \geq \frac{b^2}{4}$, which corresponds to the range of frequencies of the standing wave that we will be considering in what follows.

Our principal theme of study will consist of the standing wave solutions of (I.1), (I.2) (that is, the solutions of (I.3), (I.4)). Our main interest is in the (spectral) stability of these waves. For future reference, we introduce the associated Hamiltonian functionals,

$$\begin{aligned} I(u) &= \left\{ \frac{1}{2} \int_{\mathbf{R}^d} |\Delta u|^2 - \frac{b}{2} \int_{\mathbf{R}^d} |\nabla u|^2 - \frac{1}{p+1} \int_{\mathbf{R}^d} |u|^{p+1} \right\}, \\ J(u) &= \left\{ \frac{1}{2} \int_{\mathbf{R}^d} |\Delta u|^2 - \frac{b}{2} \int_{\mathbf{R}^d} |u_{x_1}|^2 - \frac{1}{p+1} \int_{\mathbf{R}^d} |u|^{p+1} \right\} \end{aligned}$$

and the associated constrained minimization problems

$$\begin{cases} I(u) \rightarrow \min \\ \int_{\mathbf{R}^d} |u(x)|^2 dx = \lambda. \end{cases} \quad (\text{II.1})$$

$$\begin{cases} J(u) \rightarrow \min \\ \int_{\mathbf{R}^d} |u(x)|^2 dx = \lambda. \end{cases} \quad (\text{II.2})$$

The solutions of these problems, if they exist, are referred to as normalized waves for the corresponding variational problems.

For the rest of the paper, we consider the case $b > 0$ only. We have the following result.

Theorem 1. *(The isotropic case) Let $d \geq 2$ and $b > 0$. Then, there exists a unique $p_*(d) \in (1 + \frac{4}{d}, 1 + \frac{8}{d+1})$, so that*

- For $1 < p < p_*(d)$, the constrained minimization problem (II.1) has a solution for every $\lambda > 0$. Moreover, such solutions satisfy the Euler-Lagrange equation

$$\Delta^2 \Phi + b\Delta \Phi + \omega \Phi - |\Phi|^{p-1} \Phi = 0, x \in \mathbf{R}^d, \quad (\text{II.3})$$

for some $\omega = \omega(\lambda) > 0$. In addition, all the functions $e^{-i\omega(\lambda)t} \Phi$ are spectrally stable in the context of the isotropic NLS (I.1).

- For $1 + \frac{8}{d} > p > p_*(d)$, there exists $\lambda_*(p, d, b) > 0$, so that the problem (II.1) has solutions for all $\lambda > \lambda_*(p, d)$. These solutions are spectrally stable.

Our numerical results suggest that $3.2 < p_*(2) < 3.4$, with the relevant value being in the vicinity of $p_*(2) \approx 3.3$, yet the subtle nature of the numerical considerations near the limit only affords us an approximate result in this context.

Next, we have the following result regarding the anisotropic case.

Theorem 2. *(The anisotropic case) Let $d \geq 2$ and $b > 0$. Then,*

- For $1 < p < 1 + \frac{4}{d}$, the constrained minimization problem (II.2) has a solution for every $\lambda > 0$. Moreover, all of these solutions are spectrally stable.
- For $1 + \frac{8}{d} > p > 1 + \frac{4}{d}$, there exists $\lambda_*(p, d, b) > 0$, so that the problem (II.1) has solutions for all $\lambda > \lambda_*(p, d)$. These solutions are spectrally stable.

Remark: The statement of the Theorem 2 does not imply that *all* waves are spectrally stable, but rather only that the minimizers of the constrained minimization problem (II.2) are guaranteed to be spectrally stable. In fact, in later sections, we numerically explore waves (i.e. functions satisfying (I.4)), which are not necessarily spectrally stable. Interestingly they happen to co-exist with stable constrained minimizers in that for a range of p , there exist multiple solutions corresponding to different frequencies with some (2) of them being stable and one unstable. We now turn to the systematic construction of the waves of interest.

² However, there are fourth order differential operators with fast decaying potentials, who have embedded eigenvalues in its continuous spectrum. This is in sharp contrast with the second order operators, who may possess eigenvalues only at the edges of the continuous spectrum.

III. CONSTRUCTION OF THE WAVES: PRELIMINARIES

We begin our considerations with an analysis of when the constrained minimization problem (II.1) is well-posed. That is, whether the quantity $I[u]$ is bounded from below.

A. Well-posedness of the constrained minimization problems

To this end, introduce the following functions

$$m(\lambda) = \inf_{\|u\|_{L^2}^2 = \lambda} \left\{ \frac{1}{2} \int_{\mathbf{R}^d} |\Delta u|^2 - \frac{b}{2} \int_{\mathbf{R}^d} |\nabla u|^2 - \frac{1}{p+1} \int_{\mathbf{R}^d} |u|^{p+1} \right\}$$

$$n(\lambda) = \inf_{\|u\|_{L^2}^2 = \lambda} \left\{ \frac{1}{2} \int_{\mathbf{R}^d} |\Delta u|^2 - \frac{b}{2} \int_{\mathbf{R}^d} |u_{x_1}|^2 - \frac{1}{p+1} \int_{\mathbf{R}^d} |u|^{p+1} \right\}$$

It is not *a priori* clear that $m(\lambda), n(\lambda)$ is finite. We have the following result detailing that.

Lemma 1. *Let $d \geq 1$. Then, for every $\lambda > 0$ and $1 < p < 1 + \frac{8}{d}$, we have that $-\infty < m(\lambda) < 0$.*

For $p > 1 + \frac{8}{d}$, $m(\lambda) = -\infty$.

Proof. Assume that $1 < p < 1 + \frac{8}{d}$. By the Gagliardo-Nirenberg-Sobolev's inequalities

$$\|u\|_{L^{p+1}(\mathbf{R}^d)} \leq C \|u\|_{\dot{H}^{d(\frac{1}{2} - \frac{1}{p+1})}} \leq C_{d,p} \|\Delta u\|_{L^2}^{\frac{d}{2}(\frac{1}{2} - \frac{1}{p+1})} \|u\|_{L^2}^{1 - \frac{d}{2}(\frac{1}{2} - \frac{1}{p+1})}.$$

Thus, for a function $u : \|u\|^2 = \lambda$, we have

$$\|u\|_{L^{p+1}(\mathbf{R}^d)}^{p+1} \leq \lambda^{\frac{1}{2}(p+1 - \frac{d}{4}(p-1))} \|\Delta u\|_{L^2}^{\frac{d(p-1)}{4}} =: C_\lambda \|\Delta u\|_{L^2}^{\frac{d(p-1)}{4}}.$$

Since $\frac{d(p-1)}{4} < 2$, we conclude by Young's inequality that for every $\delta > 0$,

$$\|u\|_{L^{p+1}(\mathbf{R}^d)}^{p+1} \leq \left(\frac{C_\lambda}{\delta} \right)^{\frac{8}{8-d(p-1)}} + \delta \|\Delta u\|_{L^2}^2 \leq D_{\lambda,\delta,p} + \delta \|\Delta u\|_{L^2}^2.$$

Trivially, $\|\nabla u\|^2 \leq C_d \|\Delta u\| \|u\| \leq \delta \|\Delta u\|^2 + \frac{C_d^2 \lambda}{\delta}$, so by setting $\delta = \delta_{\lambda,p,b}$ appropriately small, we obtain that for a function $u : \|u\|^2 = \lambda$,

$$I[u] \geq \frac{1}{4} \|\Delta u\|_{L^2}^2 - C_{\lambda,p,b}. \quad (\text{III.1})$$

whence the function m is bounded from below.

Let ϕ be a test function, $\|\phi\|_{L^2}^2 = \lambda$. We take the scaling transformation $\phi_a = a^{d/2} \phi(ax)$, so $\|\phi_a\|_{L^2}^2 = \lambda$. We have

$$I[\phi_\varepsilon] = a^4 \frac{\|\Delta \phi\|^2}{2} - b a^2 \frac{\|\nabla \phi\|^2}{2} - \frac{a^{\frac{d(p+1)}{2} - d}}{p+1} \|\phi\|_{L^{p+1}}^{p+1}.$$

Clearly, if $b > 0$ and $0 < a \ll 1$, the dominant term is $-b a^2 \frac{\|\nabla \phi\|^2}{2} - \frac{a^{\frac{d(p+1)}{2} - d}}{p+1} \|\phi\|_{L^{p+1}}^{p+1} < 0$, whence $m(\lambda) < 0$ for these values.

On the other hand, if $p > 1 + \frac{8}{d}$, we have $\frac{d(p+1)}{2} - d > 4$, so that $\lim_{a \rightarrow +\infty} I[\phi_a] = -\infty$. \square

The next lemmata are technical statements, which will however impact the restrictions one must impose on p (and other parameters), in order to be able to construct the waves in Theorem 1. In fact, we shall need specific Gagliardo-Nirenberg-Sobolev (GNS) type inequalities in order to resolve the existence requirements in Theorem 1 and Theorem 2.

B. The Gagliardo-Nirenberg-Sobolev inequalities with mixed dispersion

We start with the isotropic case.

Proposition 1. *Let $b > 0$. For every $d \geq 2$, there exists $p_*(d)$, so that: for all $1 < p \leq p_*(d)$, the following estimate*

$$\|\phi\|_{L^{p+1}(\mathbf{R}^d)}^{p+1} \leq C \|\phi\|_{L^2}^{p-1} \left(\int_{\mathbf{R}^d} [|\Delta\phi|^2 - b|\nabla\phi|^2 + \frac{b^2}{4}\phi^2] dx \right) \quad (\text{III.2})$$

cannot hold for a given constant C and all test functions ϕ . In addition, $p_(d)$ obeys the following*

$$1 + \frac{4}{d} \leq p_*(d) \leq 1 + \frac{8}{d+1}. \quad (\text{III.3})$$

On the other hand, for $1 + \frac{8}{d} > p > p_(d)$, there exists a constant $C = C_{p,d,b}$, so that*

$$\|\phi\|_{L^{p+1}(\mathbf{R}^d)}^{p+1} \leq C_{p,d,b} \|\phi\|_{L^2}^{p-1} \left(\int_{\mathbf{R}^d} [|\Delta\phi|^2 - b|\nabla\phi|^2 + \frac{b^2}{4}\phi^2] dx \right) \quad (\text{III.4})$$

Remark: The value of $p_*(1) = 5$ was computed in [16]. Finding the exact value of $p_*(d)$, $d \geq 2$ appears to be a hard problem in Fourier analysis, closely related to the restriction conjecture. Even in our proof of the upper bound in (III.3), we use the full strength of the Stein-Tomas restriction theorem in two spatial dimensions (see for example p. 784, [25]) which does not appear to be enough to determine $p_*(d)$. Proposition 1 allows us to prove Theorem 1; see Section IV below.

Next, we present the relevant GNS results (or lack thereof) in the anisotropic case. The result is much more definite than its counterpart Proposition 1.

Proposition 2. *Let $b > 0$. For every $d \geq 2$, and for all $1 < p \leq 1 + \frac{4}{d}$, the following estimate*

$$\|\phi\|_{L^{p+1}(\mathbf{R}^d)}^{p+1} \leq C \|\phi\|_{L^2}^{p-1} \left(\int_{\mathbf{R}^d} [|\Delta\phi|^2 - b|\partial_{x_1}\phi|^2 + \frac{b^2}{4}\phi^2] dx \right) \quad (\text{III.5})$$

cannot hold for a given constant C and all test functions ϕ .

On the other hand, for $1 + \frac{8}{d} > p > 1 + \frac{4}{d}$, there exists a constant $C = C_{p,d,b}$, so that

$$\|\phi\|_{L^{p+1}(\mathbf{R}^d)}^{p+1} \leq C_{p,d} \|\phi\|_{L^2}^{p-1} \left(\int_{\mathbf{R}^d} [|\Delta\phi|^2 - b|\partial_{x_1}\phi|^2 + \frac{b^2}{4}\phi^2] dx \right) \quad (\text{III.6})$$

In the remainder of this section, we present some preparatory material for the proofs of Proposition 1 and Proposition 2. To this end, we use the formula for the Fourier transform and its inverse as follows

$$\hat{f}(\xi) = (2\pi)^{-d/2} \int_{\mathbf{R}^d} f(x) e^{-ix \cdot \xi} dx, \quad f(x) = (2\pi)^{-d/2} \int_{\mathbf{R}^d} \hat{f}(\xi) e^{ix \cdot \xi} d\xi$$

The Plancherel's theorem states that $\|f\|_{L^2} = \|\hat{f}\|_{L^2}$. We will also make frequent use of the Bernstein inequality: for every $1 \leq p \leq q \leq \infty$ and every finite volume set $A \subset \mathbf{R}^d$, there exists $C = C_d$, so that

$$\|P_A f\|_{L^q} \leq C |A|^{\frac{1}{p} - \frac{1}{q}} \|f\|_{L^p}.$$

where $\widehat{P_A f}(\xi) = \chi_A(\xi) \hat{f}(\xi)$.

We are now ready to proceed to the specifics of the isotropic case.

C. Proof of Proposition 1

In consideration of the estimates (III.4), one can straightforwardly rescale to the case $b = 2$, which we will henceforth use in our considerations for simplicity (although when completing the proof of our theorems in section IV below, we will present them for arbitrary b). Using Fourier transformation and Plancherel's theorem, we can rewrite

$$\int_{\mathbf{R}^d} [|\Delta\phi|^2 - 2|\nabla\phi|^2 + \phi^2] dx = \int_{\mathbf{R}^d} |\hat{f}(\xi)|^2 (|\xi|^2 - 1)^2 d\xi.$$

Further, one can use smooth decompositions near $|\xi| = 1$ to study (III.4). More concretely, introduce a function $\psi \in C_0^\infty(\mathbf{R})$, so that $\psi(z) = 1, |z| < 1$ and $\psi(z) = 0, |z| > 2$. Then, let $\chi(z) = \psi(z) - \psi(2z)$, so that $\text{supp}\chi \subset (\frac{1}{2}, 2)$ and $\sum_{j=-\infty}^\infty \chi(2^j z) = 1, z \neq 0$. Now, introduce two multipliers

$$\widehat{Q_j f}(\xi) := \chi(2^{-j}(|\xi|^2 - 1))\widehat{f}(\xi), \widehat{P_m f}(\xi) := \chi(2^m(|\xi|^2 - 1))\widehat{f}(\xi),$$

and the corresponding versions $Q_{>j} := \sum_{l>j} Q_l$, $Q_{\sim j} = Q_{j-1} + Q_j + Q_{j+1}$ and so on. Based on the relevant decomposition,

$$Id = \sum_{j=0}^\infty Q_j + \sum_{m>0} P_m,$$

and $Q_j, j \geq 3$ Fourier restricts to a region $|\xi| \sim 2^{j/2}$. We henceforth adopt the notation, $A \sim B$, for two positive quantities that satisfy if $\frac{1}{4}A \leq B \leq 4A$.

It is actually not hard to come up with necessary and sufficient conditions on p so that (III.4) holds, where f is replaced by $Q_{>3}f$.

1. Estimates away from $|\xi| = 1$

We can estimate by Sobolev embedding (or rather Bernstein inequality)

$$\|Q_j f\|_{L^{p+1}(\mathbf{R}^d)}^{p+1} \leq C 2^{j \frac{(p-1)d}{4}} \|Q_j f\|_{L^2(\mathbf{R}^d)}^{p+1}. \quad (\text{III.7})$$

Computing the right-hand side of (III.4) (with $b = 2$), on the other hand, yields $2^{2j} \|Q_j f\|_{L^2(\mathbf{R}^d)}^{p+1}$. One can now show (III.4) for $Q_{>3}f$, when $1 < p < 1 + \frac{8}{d}$. Indeed, by the triangle inequality, (III.7)

$$\begin{aligned} \|Q_{>3}f\|_{L^{p+1}(\mathbf{R}^d)} &\leq C \sum_{j>3} 2^{j \frac{(p-1)d}{4(p+1)}} \|Q_j f\|_{L^2(\mathbf{R}^d)} \leq C \|f\|_{L^2}^{\frac{p-1}{p+1}} \left(\sum_{j>3} \|Q_j f\|_{L^2}^2 2^{j \frac{(p-1)d}{4}} \right)^{\frac{1}{p+1}} \leq C \|f\|_{L^2}^{\frac{p-1}{p+1}} \left(\sum_{j>3} \|Q_j f\|_{L^2}^2 2^{2j} \right)^{\frac{1}{p+1}} \\ &\leq C \|f\|_{L^2}^{\frac{p-1}{p+1}} \left(\int_{\mathbf{R}^d} [|\Delta f|^2 - 2|\nabla f|^2 + f^2] dx \right)^{\frac{1}{p+1}}. \end{aligned}$$

where we have used $\frac{(p-1)d}{4} < 2$ and $\|\xi|^2 - 1 \sim 2^j$ on the support of the multiplier Q_j .

The situation is much more delicate for frequencies close to the sphere $|\xi| = 1$, that is for the multipliers $P_m, m \gg 1$.

2. Estimates near $|\xi| = 1$

Clearly, one has, by Bernstein inequalities, the estimates $\|P_m f\|_{L^{p+1}} \leq C_m \|f\|_{L^2}$, so the issue is the control of $P_{>m}$ for a fixed m . We claim that the central issue here is the exact bound in the estimate $\|P_m f\|_{L^{p+1}(\mathbf{R}^d)} \leq C \|f\|_{L^2}$. More precisely, define

$$\alpha(p, d) = \sup \{ \alpha : \limsup_{m \rightarrow \infty} \sup_{\|f\|_{L^2} = 1} 2^{\alpha m} \|P_m f\|_{L^{p+1}(\mathbf{R}^d)} < \infty \}. \quad (\text{III.8})$$

Note that by the uniform boundedness principle and the definition of $\alpha(p, d)$, for every $\beta > \alpha(p, d)$, there is a $f_\beta : \|f_\beta\|_{L^2} = 1$, so that

$$\limsup_{m \rightarrow \infty} 2^{\beta m} \|P_m f_\beta\|_{L^{p+1}(\mathbf{R}^d)} = \infty. \quad (\text{III.9})$$

For convenience, we drop the dependence on the dimension d in $\alpha(p, d)$. Note that by the Bernstein's inequality $\alpha(p) > 0$, in fact $\|P_m f\|_{L^{p+1}} \leq C 2^{-m(\frac{1}{2} - \frac{1}{p+1})} \|f\|_{L^2}$, whence $\alpha(p, d) \geq (\frac{1}{2} - \frac{1}{p+1})$. For the same reasons, it is clear that $p \rightarrow \alpha(p)$ is an increasing function. In addition $p \rightarrow \alpha(p)$ is a continuous function and $\alpha(1) = 0$.

A convenient characterization of $\alpha(p, d)$ is the following: for every $\epsilon > 0$, there is C_ϵ , so that

$$\|P_m f\|_{L^{p+1}(\mathbf{R}^d)} \leq C_\epsilon 2^{(-\alpha(p, d) + \epsilon)m} \|f\|_{L^2(\mathbf{R}^d)}. \quad (\text{III.10})$$

We claim that $\alpha(p, d)$ determines the value of $p_*(d)$ in Proposition 1.

In fact, we claim that $p_*(d)$ is the unique solution of the equation $\alpha(p, d) = \frac{2}{p+1}$. We now prove this claim. First, we show that this equation has a unique solution. To start with, the continuous function $h(p) := \alpha(p) - \frac{2}{p+1}$ is increasing, with $h(1) = -1 < 0$, while $h(p) \geq \frac{1}{2} - \frac{3}{p+1} > 0$ for $p \geq 5$, so there will be a solution $p \in (1, 5)$. In fact, below we show better bounds on $\alpha(p, d)$, which imply existence of solutions in the interval of interest, namely $(1, 1 + \frac{8}{d})$, but the existence of solutions anywhere in $(1, \infty)$ will suffice for now.

Next, we show that for $p < p_*(d)$, (III.2) holds. This means that $\alpha(p) - \frac{2}{p+1} < 0$. Introduce $\beta > \alpha(p)$, so that $\beta < \frac{2}{p+1}$. According to the remarks made earlier, this allows us to find a function $f_\beta : \|f_\beta\|_{L^2} = 1$, so that (III.9) holds true. Assume then, for a contradiction, that (III.2) holds for some constant C . This means that for all $\phi \neq 0$,

$$\frac{\|\phi\|_{L^{p+1}}}{\|\phi\|_{L^2}^{\frac{p-1}{p+1}} \left(\int [|\Delta\phi|^2 - 2|\nabla\phi|^2 + \phi^2] dx \right)^{\frac{1}{p+1}}} \leq C. \quad (\text{III.11})$$

In particular, taking into account the properties of P_m and our earlier calculations with regards to the quantity in the denominator of (III.11), we can take $\phi_m = P_m f_\beta$,

$$\sup_m \frac{\|P_m f_\beta\|_{L^{p+1}}}{\|P_m f_\beta\|_{L^2} 2^{-\frac{2m}{p+1}}} \leq C. \quad (\text{III.12})$$

Now, since $\|P_m f_\beta\|_{L^2} \leq \|f_\beta\|_{L^2} = 1$, it follows that $\sup_m \|P_m f_\beta\|_{L^{p+1}} 2^{\frac{2m}{p+1}} \leq C$. But this is a contradiction with (III.9), since

$$\|P_m f_\beta\|_{L^{p+1}} 2^{\beta m} 2^{m(\frac{2}{p+1} - \beta)} = \|P_m f_\beta\|_{L^{p+1}} 2^{\frac{2m}{p+1}} \leq C,$$

whereas on the left hand side $\limsup_m \|P_m f_\beta\|_{L^{p+1}} 2^{\beta m} = \infty$, and $\lim_m 2^{m(\frac{2}{p+1} - \beta)} = \infty$.

Assume now $p > p_*(d)$, so $\alpha(p) > \frac{2}{p+1}$. So, we can find $\beta : \alpha(p) > \beta > \frac{2}{p+1}$. Then, we have the estimate, (see (III.10)), but applied to $P_m^2 f$

$$\|P_m f\|_{L^{p+1}(\mathbf{R}^d)} \leq C_e 2^{-\beta m} \|P_m f\|_{L^2(\mathbf{R}^d)}. \quad (\text{III.13})$$

We will show that (III.4) holds. In view of the estimates away from $|\xi| = 1$, which establish (III.4) for $Q_{>3}f$, it suffices to consider $P_{>m_0}f$ for m_0 sufficiently large only. We take $m_0 = 10$ for concreteness. By (III.13), we have

$$\begin{aligned} \|P_{>10}f\|_{L^{p+1}} &\leq \sum_{m>10} \|P_m f\|_{L^{p+1}} \leq C \sum_{m>10} 2^{-\beta m} \|P_m f\|_{L^2} \leq C \|f\|_{L^2}^{\frac{p-1}{p+1}} \left(\sum_{m>10} \|P_m f\|_{L^2}^2 2^{-2m} \right)^{\frac{1}{p+1}} \leq \\ &\leq C \|f\|_{L^2}^{\frac{p-1}{p+1}} \left(\int [|\Delta f|^2 - 2|\nabla f|^2 + f^2] dx \right)^{\frac{1}{p+1}}. \end{aligned}$$

This establishes (III.4) and so the estimates (or lack thereof) in Proposition 1 are established in full.

We now focus our attention on appropriate estimates on $p_*(d)$.

3. Estimates on the value of $p_*(d)$

As we saw above, the value $p_*(d)$ is intimately related to the precise estimates of $P_m : L^2(\mathbf{R}^d) \rightarrow L^{p+1}(\mathbf{R}^d)$. Recall that there was the trivial bound based on the Bernstein's inequality, $\alpha(p, d) \geq (\frac{1}{2} - \frac{1}{p+1})$, but we now aim for a much more sophisticated one. Before we proceed, we need to introduce some quantities that will be helpful in our considerations. The surface measure on \mathbf{S}^{d-1} is defined via $d\sigma(x) = \delta(|x|^2 - 1)$ and its Fourier transform is (see [25], Appendix B.4)

$$\widehat{d\sigma}(\xi) = (2\pi)^{-d/2} \int_{\mathbf{S}^{d-1}} e^{-i\xi \cdot \theta} d\theta = c_d \frac{J_{\frac{d-2}{2}}(|\xi|)}{|\xi|^{\frac{d-2}{2}}} =: S(\xi).$$

where c_d is a constant and J_n are the standard Bessel functions. Furthermore, see Appendix B.5, [25], for any radial function $f(x) = f_0(|x|)$, one can compute its Fourier transform as follows

$$\hat{f}(\xi) = C_d |\xi|^{-\frac{d-2}{2}} \int_0^\infty f_0(r) J_{\frac{d-2}{2}}(r|\xi|) r^{\frac{d}{2}} dr.$$

In this way, when we take the multipliers associated to P_m , namely $f_0(r) = \chi(2^m(r^2 - 1))$, we see that its kernel K_m (i.e., $P_m f = f * K_m$) can be expressed in terms of an averaging operator involving the kernel $S = \widehat{d\sigma}$ as follows

$$K_m(x) = C_d \int_0^\infty \chi(2^m(r^2 - 1)) \frac{J_{\frac{d-2}{2}}(r|x|)}{|x|^{\frac{d-2}{2}}} r^{\frac{d}{2}} dr = C_d \int_0^\infty \chi(2^m(r^2 - 1)) r^{d-1} S(r|x|) dr.$$

Let us now fix $q > 2$. We wish to establish an estimate for the operator norm $P_m : L^2 \rightarrow L^q$. Note that P_m is trivially bounded, but the issue is to determine precise bounds on the norm, as a function of m . Due to the fact that χ is real-valued, $P_m : L^{q'} \rightarrow L^2$, so in order to compute $\|P_m\|_{B(L^2 \rightarrow L^q)}$, we might instead consider $P_m^2 : L^{q'} \rightarrow L^q$ and in addition

$$\|P_m\|_{B(L^2 \rightarrow L^q)} = \sqrt{\|P_m^2\|_{B(L^{q'} \rightarrow L^q)}}.$$

Now, $P_m^2 f = \tilde{K}_m * f$, $\tilde{K}_m = C_d \int_0^\infty \chi^2(2^m(r^2 - 1)) r^{d-1} S(r|x|) dr$. The advantage in this formulation is that the mapping properties of the operator $f \rightarrow f * \widehat{d\sigma} = f * S$ are well-understood. In fact, this is the content of the celebrated Stein-Tomas theorem. To summarize, (see (10.4.7), p. 784, [25]), there is the estimate

$$\|f * S\|_{L^q(\mathbb{R}^d)} \leq C \|f\|_{L^{q'}(\mathbb{R}^d)}, \quad q_d = \frac{2(d+1)}{d-1} \quad (\text{III.14})$$

With this value of q_d , we then conclude that since $f * \tilde{K}_m = C_d \int_0^\infty \chi^2(2^m(r^2 - 1)) r^{d-1} [S(r|\cdot|) * f] dr$, we have the estimate, based on the Stein-Tomas bound (III.14),

$$\|P_m^2 f\|_{L^q} = \|f * \tilde{K}_m\|_{L^q} \leq C 2^{-m} \|f\|_{L^{q'}}.$$

Note here that the factor 2^{-m} is gained through the integration in r , while the estimate for the term $\|[S(r|\cdot|) * f]\|_{L^q}$ comes from (III.14). Accordingly, this gives the estimate

$$\|P_m f\|_{L^{q_d}} \leq C 2^{-m/2} \|f\|_{L^2}, \quad q_d = \frac{2(d+1)}{d-1}. \quad (\text{III.15})$$

Interpolating this estimate with the trivial one $\|P_m f\|_{L^2} \leq C \|f\|_{L^2}$, we conclude that for every $2 \leq q \leq \frac{2(d+1)}{d-1}$, there is

$$\|P_m f\|_{L^q} \leq C 2^{-m \frac{d+1}{2} \left(\frac{1}{2} - \frac{1}{q}\right)} \|f\|_{L^2}. \quad (\text{III.16})$$

It follows that

$$\alpha(p, d) \geq \frac{d+1}{2} \left(\frac{1}{2} - \frac{1}{p+1} \right). \quad (\text{III.17})$$

In particular, it is clear that $\alpha(p, d) - \frac{2}{p+1} > 0$, if $p > 1 + \frac{8}{d+1}$, which means that we have established the upper bound $p_*(d) < 1 + \frac{8}{d+1}$.

In order to establish the lower bound for $p_*(d)$, we test the ratio $\frac{\|P_m f\|_{L^r(\mathbb{R}^d)}}{\|f\|_{L^2(\mathbb{R}^d)}}$ for $r > 2$, with $f = K_m$, defined above. For the correct asymptotics, we need to recall (see Appendix B.6, [25]) that for every $r \gg 1$,

$$J_k(r) = c \frac{\cos\left(r - \frac{\pi k}{2} - \frac{\pi}{4}\right)}{\sqrt{r}} + O(r^{-3/2}).$$

Now,

$$\begin{aligned} \tilde{K}_m(x) &= C_d \int_0^\infty \chi^2(2^m(r^2 - 1)) r^{d-1} S(r|x|) dr \\ &= \text{const.} |x|^{-\frac{d-1}{2}} \int_0^\infty \chi^2(2^m(r^2 - 1)) r^{d-1} \frac{\cos\left(r|x| - \frac{\pi(d-2)}{4} - \frac{\pi}{4}\right)}{r^{\frac{d-1}{2}}} dr + 2^{-m} O(|x|^{-\frac{d+1}{2}}). \end{aligned}$$

It is then easy to see that for $2^{-m} \ll \delta \ll 1$ and $|x| \sim \delta 2^m$, $m \gg 1$, in the integral above there is the approximate formula

$$\cos\left(r|x| - \frac{\pi(d-2)}{4} - \frac{\pi}{4}\right) = \cos\left(|x| - \frac{\pi(d-2)}{4} - \frac{\pi}{4}\right) + O(\delta).$$

This implies that for a fixed portion of the set $|x| \sim \delta 2^m$, $\cos(r|x| - \frac{\pi(d-2)}{4} - \frac{\pi}{4}) \geq \frac{1}{2}$, whence we have that \tilde{K}_m obeys, on this fixed portion of the set, the bound $|\tilde{K}_m(x)| \gtrsim 2^{-m\frac{d+1}{2}}$. Thus,

$$\|P_m f\|_{L^r(\mathbf{R}^d)} \geq c 2^{-\frac{m}{2}} 2^{-md(\frac{1}{2}-\frac{1}{r})}$$

while by Plancherel's theorem

$$\|f\|_{L^2} = \|\mathcal{K}_m\|_{L^2} = \left(\int_{\mathbf{R}^d} |\chi(2^m(|\xi|^2 - 1))|^2 d\xi \right)^{\frac{1}{2}} \sim 2^{-\frac{m}{2}}.$$

Thus,

$$\frac{\|P_m f\|_{L^r(\mathbf{R}^d)}}{\|f\|_{L^2(\mathbf{R}^d)}} \geq c 2^{-md(\frac{1}{2}-\frac{1}{r})}.$$

It follows that one has the inequality complementary to (III.17),

$$\alpha(p, d) \leq d \left(\frac{1}{2} - \frac{1}{p+1} \right). \quad (\text{III.18})$$

We can now derive an estimate for $p_*(d)$. Indeed,

$$\alpha(p, d) - \frac{2}{p+1} \leq d \left(\frac{1}{2} - \frac{1}{p+1} \right) - \frac{2}{p+1} < 0,$$

if $p < 1 + \frac{4}{d}$. Thus, we conclude that $p_*(d) > 1 + \frac{4}{d}$. This finishes the proof of Proposition 1.

Our next goal is to analyze the relevant GNS inequalities in the non-isotropic case.

D. The anisotropic case: Proof of Proposition 2

Again, a simple rescaling argument reduces matters to the case $b = 2$, as in the proof of Proposition 1. The arguments for the anisotropic case are pretty similar, once we realize the important differences in the dispersion relations. More specifically, using Plancherel's theorem in this case:

$$\int_{\mathbf{R}^d} [|\Delta\phi|^2 - 2|\partial_{x_1}\phi|^2 + |\phi|^2] dx = \int_{\mathbf{R}^d} |\hat{\phi}(\xi)|^2 [(\xi_1^2 - 1)^2 + |\xi'|^4 + 2\xi_1^2|\xi'|^2] d\xi,$$

where $\xi' = (\xi_2, \dots, \xi_d)$. For future reference, introduce the dispersion related function $h(\xi) := (\xi_1^2 - 1)^2 + |\xi'|^4 + 2\xi_1^2|\xi'|^2$. Based on this formula, we discuss the validity of (III.5).

We start our analysis by considering some easy regions. One such region, is when ξ_1 is away from ± 1 . Quantitatively, $|\xi_1^2 - 1| \geq \frac{1}{100}$ and say $f_0 := P_{|\xi_1^2 - 1| \geq \frac{1}{100}} f$. In this case, we clearly have $h(\xi) \sim 1 + \xi_1^4 + |\xi'|^4 \sim \xi >^4$. In such a scenario, it is easy to analyze $\|f_0\|_{L^{p+1}(\mathbf{R}^d)}$, in particular what it takes for (III.6) to hold (and (III.5) to fail respectively).

More specifically, assuming $1 < p < 1 + \frac{8}{d}$, we have by Bernstein's inequality and Plancherel's equality

$$\begin{aligned} \|f_0\|_{L^{p+1}(\mathbf{R}^d)}^{p+1} &\leq C(\|f_0\|_{L^2} + \sum_{k=0}^{\infty} 2^{kd(\frac{1}{2}-\frac{1}{p+1})} \|P_k f_0\|_{L^2})^{p+1} \leq C\|f_0\|_{L^2}^{p-1} \sum_{k=0}^{\infty} 2^{4k} \int_{|\xi_1| \sim 2^k} |\hat{f}_0(\xi)|^2 d\xi \\ &\leq C\|f\|_{L^2}^{p-1} \int_{\mathbf{R}^d} |\hat{f}_0(\xi)|^2 h(\xi) d\xi \leq C\|f\|_{L^2}^{p-1} \int_{\mathbf{R}^d} [|\Delta f|^2 - 2|\partial_{x_1} f|^2 + |f|^2] dx. \end{aligned}$$

This shows that $1 < p < 1 + \frac{8}{d}$ is a sufficient condition for the validity of (III.6), in the case, where ξ_1 is away from ± 1 . On the other hand, testing (III.6) with a function of the type $\hat{f}(\xi) = \varphi(2^{-k}\xi)$ for $k \gg 1$, shows that $1 < p < 1 + \frac{8}{d}$ is necessary as well.

We now turn our attention to the more interesting cases, namely $|\xi_1^2 - 1| \sim 2^{-m}$, $m \gg 1$. In this case,

$$h(\xi) \sim 2^{-2m} + |\xi'|^4 + |\xi'|^2.$$

The case $|\xi'| \geq \frac{1}{100}$ reduces to $h(\xi) \sim \xi >^4$, which was just analyzed. So, it remains to consider the cases $|\xi'| < \frac{1}{100}$. So, the dispersion relation will be exactly $h(\xi) \sim 2^{-2m} + |\xi'|^2$. Further, by changing the Fourier variables $\xi_1 \rightarrow \xi_1 \pm 1$ (which on

the physical side means replacing f with $f \rightarrow e^{\bar{i}x_1} f$, a harmless operation in terms of all $\|\cdot\|_{L^q}$ norms), we are reduced to studying the question: for which values of p can the inequality hold

$$\|f\|_{L^{p+1}}^{p+1} \leq C \|f\|_{L^2}^{p-1} \int_{\mathbf{R}^d} |\hat{f}(\xi)|^2 |\xi|^2 d\xi, \quad (\text{III.19})$$

where f is a function $\text{supp } \hat{f} \subset \{\xi : |\xi| \ll 1\}$.

We will now show that $p \geq 1 + \frac{4}{d}$ is a necessary and sufficient condition for (III.19) to hold. We have already established that $1 + \frac{8}{d} > p$ is necessary and sufficient for the region away from $\xi_1 = \pm 1$, which will of course need to be intersected with the necessary and sufficient condition for (III.19) to hold.

To this end, assume that $p \geq 1 + \frac{4}{d}$. Consider $f = \sum_{k=0}^{\infty} P_{-k} f$ (recall $\text{supp } \hat{f} \subset \{\xi : |\xi| \ll 1\}$), so by standard properties of the Littlewood-Paley decompositions and the Bernstein's inequality

$$\|f\|_{L^{p+1}(\mathbf{R}^d)}^2 \leq C \sum_{k=0}^{\infty} \|P_{-k} f\|_{L^{p+1}(\mathbf{R}^d)}^2 \leq C \sum_{k=0}^{\infty} 2^{-2kd(\frac{1}{2} - \frac{1}{p+1})} \|P_{-k} f\|_{L^2(\mathbf{R}^d)}^2.$$

Further applying Cauchy-Schwartz

$$\begin{aligned} \|f\|_{L^{p+1}(\mathbf{R}^d)}^2 &\leq C \left(\sum_{k=0}^{\infty} \|P_{-k} f\|_{L^2}^2 \right)^{\frac{p-1}{p+1}} \left(\sum_k 2^{-2kd(\frac{1}{2} - \frac{1}{p+1})\frac{p+1}{2}} \|P_{-k} f\|_{L^2(\mathbf{R}^d)}^2 \right)^{\frac{2}{p+1}} \\ &\leq C \|f\|_{L^2}^{\frac{p-1}{p+1}} \left(\sum_k 2^{-kd\frac{p-1}{2}} \|P_{-k} f\|_{L^2(\mathbf{R}^d)}^2 \right)^{\frac{2}{p+1}}. \end{aligned}$$

It follows that whenever $p \geq 1 + \frac{4}{d}$, we have

$$\|f\|_{L^{p+1}}^{p+1} \leq C \|f\|_{L^2}^{p-1} \sum_{k=0}^{\infty} 2^{-2k} \|P_{-k} f\|_{L^2(\mathbf{R}^d)}^2 \leq C \|f\|_{L^2}^{p-1} \int_{\mathbf{R}^d} |\hat{f}(\xi)|^2 |\xi|^2 d\xi.$$

This establishes (III.19) under the assumption $p \geq 1 + \frac{4}{d}$. Conversely, assuming that (III.4) holds, we test it with a function $f : \hat{f}(\xi) = \chi(2^k(\xi_1 - 1), 2^k \xi')$, $k \gg 1$. This yields the inequality $p \geq 1 + \frac{4}{d}$. Thus, we have finally established that the necessary and sufficient condition for (III.6) to hold is exactly $1 + \frac{8}{d} > p \geq 1 + \frac{4}{d}$.

IV. COMPLETION OF THE PROOFS OF THEOREM 1 AND THEOREM 2

We start our presentation with the proof for the existence of the waves. Along the way, we establish a few necessary spectral properties of the corresponding linearized operators, which will be instrumental in the spectral stability considerations.

A. Existence of the waves - isotropic case

In this section, we present the proofs for the existence (or at least a very detailed scheme of the proof) for the isotropic case. We start with a few words about strategy, even though our approach, in principle, is a quite natural one. It was established in Lemma 1 that the constrained minimization problem (II.1) is well-posed, and in fact $-\infty < m(\lambda) < 0$. We would like to show that there is a minimizer for this problem, which subsequently will be shown to satisfy the Euler-Lagrange equation (II.3). To this end, consider a minimizing sequence, say $\phi_k \in H^2(\mathbf{R}^d)$. Ultimately, we would like to show that a strongly convergent subsequence of ϕ_k will converge to a solution Φ . The central issue that we need to address is the non-triviality of such a minimizing sequence. This is the subject of the next technical lemma.

Lemma 2. *Let $b > 0, d \geq 2$ and $1 < p < 1 + \frac{8}{d}$. Let also*

- $1 < p \leq p^*(d)$ and $\lambda > 0$
- $p^*(d) < p < 1 + \frac{8}{d}$ and $\lambda > \lambda_{b,p,d}$.

Then, there exists a subsequence of ϕ_k so that for some $L_1 > 0, L_2 > 0, L_3 > 0$,

$$\int_{\mathbf{R}^d} |\Delta \phi_k|^2 dx \rightarrow L_1; \int_{\mathbf{R}^d} |\nabla \phi_k|^2 dx \rightarrow L_2; \int_{\mathbf{R}^d} |\phi_k|^{p+1} dx \rightarrow L_3. \quad (\text{IV.1})$$

Informally, the claim is that for $1 < p \leq p^*(d)$, $\lambda > 0$ and for $p^*(d) < p < 1 + \frac{8}{d}$, $\lambda > \lambda_{b,p,d}$ (where $\lambda_{b,p,d}$ is some threshold depending on the parameters b, p, d), one has non-trivial minimizing sequences. Note that this does not yet show the existence of a limit, for which we bring the full weight of the compensated compactness theory to bear. At the same time this rules out some of the main obstacles toward the strong convergence of, a subsequence of a translate of ϕ_k , to a minimizer.

Proof. By the estimate (III.1), it is clear that $\{\int_{\mathbf{R}^d} |\Delta \phi_k|^2 dx\}_k$ is a bounded sequence. Since $\|\phi_k\|^2 = \lambda$ is fixed, by Sobolev embedding it follows that $\int_{\mathbf{R}^d} |\nabla \phi_k|^2 dx, \int_{\mathbf{R}^d} |\phi_k|^{p+1} dx$ are bounded as well. We can take subsequences to ensure that the convergences in (IV.5) hold true.

Now, it remains to establish the non-trivial claim, namely that all L_1, L_2, L_3 are non-zero. Assume for a contradiction that $L_3 = 0$. Introduce

$$\tilde{I}[u] := \left\{ \frac{1}{2} \int_{\mathbf{R}^d} |\Delta u|^2 - \frac{b}{2} \int_{\mathbf{R}^d} |\nabla u|^2 \right\}.$$

Clearly, $\tilde{I}[u] \geq I[u]$, whereas $\lim_k \tilde{I}[\phi_k] = \lim_k I[\phi_k] = \inf_{\|u\|^2=\lambda} I[u] \leq \inf_{\|u\|^2=\lambda} \tilde{I}[u]$. It follows that ϕ_k is a minimizing sequence for the problem $\inf_{\|u\|^2=\lambda} \tilde{I}[u]$ and the minima coincide. On the other hand, by Plancherel's theorem

$$\int_{\mathbf{R}^d} |\Delta u|^2 - b \int_{\mathbf{R}^d} |\nabla u|^2 + \frac{b^2}{4} \|u\|^2 = \int_{\mathbf{R}^d} |\hat{u}(\xi)|^2 \left(|\xi|^2 - \frac{b}{2} \right)^2 d\xi \geq 0, \quad (\text{IV.2})$$

whence $\inf_{\|u\|^2=\lambda} \tilde{I}[u] \geq -\frac{b^2}{8} \lambda$. In fact, there is equality, i.e., $\inf_{\|u\|^2=\lambda} \tilde{I}[u] = -\frac{b^2}{8} \lambda$ as the inequality in (IV.2) may be saturated by choosing a function u , so that \hat{u} is supported arbitrarily close to $|\xi| = \frac{\sqrt{b}}{2}$.

All in all, it follows that $\inf_{\|u\|^2=\lambda} I[u] = -\frac{b^2}{8} \lambda$. Applying this to arbitrary $f \neq 0$, and then $u = \sqrt{\lambda} \frac{f}{\|f\|}$, so that $\|u\|^2 = \lambda$, we have

$$\frac{2\lambda^{\frac{p-1}{2}}}{p+1} \int_{\mathbf{R}^d} |f|^{p+1} \leq \|f\|^{p-1} \left\{ \int_{\mathbf{R}^d} |\Delta f|^2 - b |\nabla f|^2 + \frac{b^2}{4} |f|^2 \right\}.$$

This last inequality is in contradiction with (III.2) for $1 < p \leq p^*(d)$, and with (III.3) for all large enough λ . This completes the proof for $L_3 > 0$ under these assumptions.

Assuming that either $L_1 = 0$ or $L_2 = 0$ implies, by the standard Gagliardo-Nirenberg inequality, the fact that $L_3 = 0$, which we have just shown to be impossible. \square

The rest of the proof for existence of a minimizer proceeds identically to the one presented in Section 3.2, [16]. Namely, first one establishes that the function $\lambda \rightarrow m(\lambda)$ is strictly sub-additive for $1 < p < 1 + \frac{8}{d}$. That is, for all $\alpha \in (0, \lambda)$,

$$m(\lambda) < m(\alpha) + m(\lambda - \alpha). \quad (\text{IV.3})$$

This is standard, and proceeds via the property that $\lambda \rightarrow \frac{m(\lambda)}{\lambda}$ is a non-increasing function, which can be obtained via elementary scaling arguments and the crucial property $\lim_k \int_{\mathbf{R}^d} |\phi_k|^{p+1} = L_3 > 0$, which was established in (IV.5).

Next, taking a minimizing subsequence ϕ_k , with the property (IV.5), one applies the compensated compactness lemma to it. More specifically, by the P.L. Lions concentration compactness lemma (see Lemma 1.1, [26]), applied to $\rho_k := |\phi_k|^2 \in L^1(\mathbf{R}^d)$, $\|\rho_k\|_{L^1} = \lambda$ there is a subsequence (denoted again by ρ_k), so that at least one of the following is satisfied:

1. *Tightness.* There exists $y_k \in \mathbf{R}$ such that for any $\varepsilon > 0$ there exists $R(\varepsilon)$ such that for all k

$$\int_{B(y_k, R(\varepsilon))} \rho_k dx \geq \int_{\mathbf{R}} \rho_k dx - \varepsilon.$$

2. *Vanishing.* For every $R > 0$

$$\limsup_{k \rightarrow \infty} \sup_{y \in \mathbf{R}} \int_{B(y, R)} \rho_k dx = 0.$$

3. *Dichotomy.* There exists $\alpha \in (0, \lambda)$, such that for any $\varepsilon > 0$ there exist $R, R_k \rightarrow \infty, y_k \in \mathbf{R}^d$, such that

$$\left\{ \begin{array}{l} \left| \int_{B(y_k, R)} \rho_k dx - \alpha \right| < \varepsilon, \quad \left| \int_{R < |x - y_k| < R_k} \rho_k dx \right| < \varepsilon, \\ \left| \int_{R_k < |x - y_k|} \rho_k dx - (\lambda - \alpha) \right| < \varepsilon. \end{array} \right. \quad (\text{IV.4})$$

Then, one shows that the dichotomy cannot occur. The proof proceeds via an argument that shows that dichotomy leads to a inequality of the form $m(\lambda) \geq m(\alpha) + m(\lambda - \alpha)$, with α as in the dichotomy alternative. This of course contradicts the strict sub-additivity (IV.3). Next, vanishing leads, via the standard Gagliardo-Nirenberg's, to $\lim_k \int_{\mathbf{R}^d} |\phi_k|^{p+1} = 0$, in a contradiction with (IV.5), namely $\lim_k \int_{\mathbf{R}^d} |\phi_k|^{p+1} = L_3 > 0$.

Hence, one concludes tightness. But tightness means that for some sequence $y_k \in \mathbf{R}^d$, there is strong L^2 convergence for $\{\phi_k(x - y_k)\}$. Denote $\Phi(\cdot) := \lim_k \phi_k(\cdot - y_k)$. By the lower semi-continuity of the L^2 norm with respect to weak convergence, we also conclude that $\lim_k \|\Phi(\cdot) - \phi_k(\cdot - y_k)\|_{H^2} = 0$, whence Φ is a constrained minimizer of (II.1), all under the assumptions of Lemma 2.

Now, we take on the question for the Euler-Lagrange equation (II.3). To this end, fix a test function h and consider the scalar function

$$g(\epsilon) := I\left(\sqrt{\lambda} \frac{\Phi + \delta h}{\|\Phi + \delta h\|}\right).$$

Since g is differentiable in a neighborhood of the origin, and achieves its minimum there, we have that $g'(0) = 0$. Since this is true for all test functions h , the resulting expression is that Φ is a distributional solution of (II.3). It is standard result in elliptic theory to conclude that such a solution $\Phi \in H^4(\mathbf{R}^d)$. In addition, one can establish asymptotics for such functions, but we will not do so herein.

Next, we consider the second derivative necessary condition for a minimum at zero, which states that $g''(0) \geq 0$. Assuming that the test function $h \perp \Phi$, we conclude $\langle \mathcal{L}_+ h, h \rangle \geq 0$, which is exactly $\mathcal{L}_+|_{\{\Phi\}^\perp} \geq 0$. In fact, this is sharp, because by a direct inspection ³ $\mathcal{L}_+[\nabla\Phi] = 0$. Also, since $\langle \mathcal{L}_+ \Phi, \Phi \rangle = -(p-1) \int |\Phi|^{p+1} dx < 0$, we conclude that \mathcal{L}_+ indeed has a negative eigenvalue. This coupled with $\mathcal{L}_+|_{\{\Phi\}^\perp} \geq 0$ confirms that \mathcal{L}_+ has exactly one negative eigenvalue.

Finally, we show that $\mathcal{L}_- \geq 0$. Assume not. Then, there is $\psi \perp \Phi, \|\psi\| = 1, \mathcal{L}_- \psi = -\sigma^2 \psi$. Note however that $\mathcal{L}_- > \mathcal{L}_+$, whence

$$0 \leq \langle \mathcal{L}_+ \psi, \psi \rangle < \langle \mathcal{L}_- \psi, \psi \rangle = -\sigma^2,$$

which is a contradiction. Looking closely, this also shows that 0 is a simple eigenvalue for \mathcal{L}_- , because then, we take $\psi \perp \Phi : \mathcal{L}_- \psi = 0$, and this still leads to a contradiction as above. Thus, we have shown the following proposition.

Proposition 3. *Let $b > 0, d \geq 2, 1 < p < 1 + \frac{8}{d}$ and one of the two assumptions below are verified*

- $1 < p \leq p^*(d)$ and $\lambda > 0$
- $p^*(d) < p < 1 + \frac{8}{d}$ and $\lambda > \lambda_{b,p,d}$.

Then, there exists $\Phi = \Phi_\lambda$, a constrained minimizer of (II.1) and $\omega = \omega_\lambda > 0$. In addition, Φ satisfies the Euler-Lagrange equation (II.3), and the linearized Schrödinger operators \mathcal{L}_\pm satisfy

1. $\mathcal{L}_-[\Phi] = 0, 0 \in \sigma_{p,p}(\mathcal{L}_-)$ is a simple eigenvalue, and $\mathcal{L}_-|_{\{\Phi\}^\perp} \geq \delta > 0$, for some $\delta > 0$
2. $\mathcal{L}_+|_{\{\Phi\}^\perp} \geq 0$. Moreover, $n(\mathcal{L}_+) = 1$

This completes the existence part of Theorem 1.

B. Existence of the waves - anisotropic case

Following identical steps as in Section IV A, we establish the following analog of Lemma 2.

Lemma 3. *Let $b > 0, d \geq 2$ and $1 < p < 1 + \frac{8}{d}$. Let also*

- $1 < p \leq 1 + \frac{4}{d}$ and $\lambda > 0$
- $1 + \frac{4}{d} < p < 1 + \frac{8}{d}$ and $\lambda > \lambda_{b,p,d}$.

Then, there exists a subsequence of ϕ_k so that for some $L_1 > 0, L_2 > 0, L_3 > 0$,

$$\int_{\mathbf{R}^d} |\Delta \phi_k|^2 dx \rightarrow L_1; \int_{\mathbf{R}^d} |\nabla \phi_k|^2 dx \rightarrow L_2; \int_{\mathbf{R}^d} |\phi_k|^{p+1} dx \rightarrow L_3. \quad (\text{IV.5})$$

³ Note however that $\nabla\Phi \perp \Phi$

The proof of Lemma 3 proceeds in an identical manner to the proof of Lemma 2 in Section IV A, with the suitable replacement of isotropic Proposition 1 with its anisotropic analog Proposition 2.

Once this step is completed, one establishes the strong sub-linearity of the cost function $n(\lambda)$, similar to the sub-linearity of $m(\lambda)$. The next step, again identical to the corresponding step for the isotropic case, is to show that once we take a minimizing sequence ϕ_k , the method of compensated compactness goes through for the functions $\rho_k := \phi_k^2$. This establishes the existence of the minimizer Φ . Similarly, it satisfies the Euler-Lagrange equation and the spectral properties hold true. We collect the results in the next Proposition.

Proposition 4. *Let $b > 0, d \geq 2, 1 < p < 1 + \frac{8}{d}$ and one of the two assumptions below are verified*

- $1 < p \leq 1 + \frac{4}{d}$ and $\lambda > 0$
- $1 + \frac{4}{d} < p < 1 + \frac{8}{d}$ and $\lambda > \lambda_{b,p,d}$.

Then, there exists $\Phi = \Phi_{\lambda, \omega} = \omega_{\lambda} > 0$, a constrained minimizer of (II.2). In addition, Φ satisfies the Euler-Lagrange equation (I.4) and the linearized operators \mathcal{L}_{\pm} obey

1. $\mathcal{L}_{-} \geq 0$. More specifically, $\mathcal{L}_{-}[\Phi] = 0, 0 \in \sigma_{p,p}(\mathcal{L}_{-})$ is a simple eigenvalue, and $\mathcal{L}_{-}|_{\{\Phi\}^{\perp}} \geq \delta > 0$, for some $\delta > 0$
2. $\mathcal{L}_{+}|_{\{\Phi\}^{\perp}} \geq 0$. Moreover, $n(\mathcal{L}_{+}) = 1$.

C. Spectral stability of the normalized waves

In this section, we show the spectral stability of the waves constructed as constrained minimizers as (II.1), (II.2) respectively. Starting with the eigenvalue problem (I.5), we have that instability is equivalent to the solvability of the system

$$\begin{cases} \mathcal{L}_{-}g = -\lambda f \\ \mathcal{L}_{+}f = \lambda g \end{cases} \quad (\text{IV.6})$$

for some $\lambda : \Re \lambda > 0$. So, applying \mathcal{L}_{-} to the second equation, we see that (IV.6) reduces to the solvability of

$$\mathcal{L}_{-}\mathcal{L}_{+}f = -\lambda^2 f. \quad (\text{IV.7})$$

Conversely, if (IV.7) has a non-trivial solution λ, f , then $g := \lambda^{-1}\mathcal{L}_{+}f$ has a nontrivial solution λ, f, g . So, (IV.6) and (IV.7) are equivalent and we concentrate on the eigenvalue problem $\mathcal{L}_{-}\mathcal{L}_{+}f = -\lambda^2 f$ henceforth.

It follows immediately that $f \perp \Phi$. Thus, as $\mathcal{L}_{-}|_{\{\Phi\}^{\perp}} \geq \delta > 0$, it follows that there exists unique $\eta \in \{\Phi\}^{\perp}$, so that $f = \sqrt{\mathcal{L}_{-}}\eta$. Writing the relation $\mathcal{L}_{-}\mathcal{L}_{+}f = -\lambda^2 f$ in terms of η yields

$$\sqrt{\mathcal{L}_{-}}(\sqrt{\mathcal{L}_{-}}\mathcal{L}_{+}\sqrt{\mathcal{L}_{-}}\eta + \lambda^2\eta) = 0.$$

As $\sqrt{\mathcal{L}_{-}}\mathcal{L}_{+}\sqrt{\mathcal{L}_{-}}\eta + \lambda^2\eta \in \{\Phi\}^{\perp} = \text{Ker}(\mathcal{L}_{-})^{\perp}$, we conclude that $\sqrt{\mathcal{L}_{-}}\mathcal{L}_{+}\sqrt{\mathcal{L}_{-}}\eta + \lambda^2\eta = 0$. Thus,

$$\sqrt{\mathcal{L}_{-}}\mathcal{L}_{+}\sqrt{\mathcal{L}_{-}}\eta = -\lambda^2\eta \quad (\text{IV.8})$$

Note however that the operator $\sqrt{\mathcal{L}_{-}}\mathcal{L}_{+}\sqrt{\mathcal{L}_{-}}$ is symmetric now, whence $-\lambda^2 \in \sigma_{p,p}(\sqrt{\mathcal{L}_{-}}\mathcal{L}_{+}\sqrt{\mathcal{L}_{-}})$, so $-\lambda^2 \in \mathbf{R}$. We have already shown that there could not be oscillatory instabilities. Furthermore, testing (IV.8) with $\eta \in \{\Phi\}^{\perp}$, we obtain

$$-\lambda^2 \|\eta\|^2 = \langle \mathcal{L}_{+}\sqrt{\mathcal{L}_{-}}\eta, \sqrt{\mathcal{L}_{-}}\eta \rangle = \langle \mathcal{L}_{+}f, f \rangle.$$

Since $f \in \{\Phi\}^{\perp}$ and $\mathcal{L}_{+}|_{\{\Phi\}^{\perp}} \geq 0$, it follows that $\langle \mathcal{L}_{+}f, f \rangle \geq 0$, whence $-\lambda^2 \geq 0$. This implies that all spectrum is stable, hence the spectral stability of Φ follows.

V. NUMERICAL COMPUTATIONS

In the present section, we show a number of numerical computations for $d = 2$ which corroborate and complement our analytical results on the existence and stability of solitons for both the isotropic and anisotropic models with competing Laplacian and biharmonic operators.

We start with the isotropic case. A summary of our results can be firstly found in Fig. 1 which contains a two-parameter (p vs b) diagram. Here, the depicted curve separates the regime of spectrally stable waves (under the curve) from spectrally

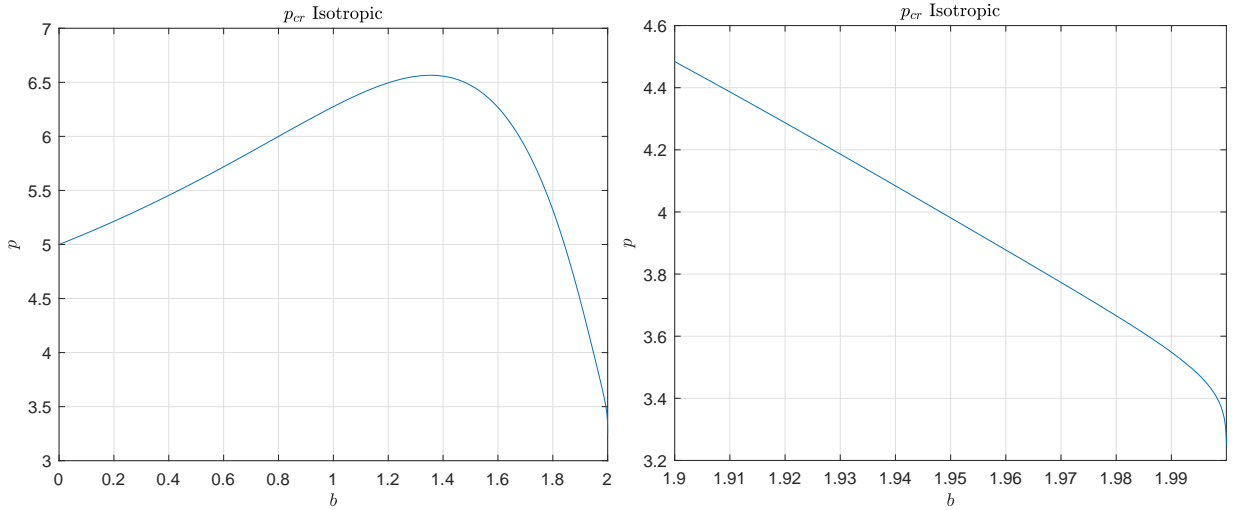


FIG. 1. Two-parameter plane of the nonlinearity exponent parameter p vs. the Laplacian prefactor b (varying between 0 and 2); recall that the frequency ω is fixed to unity, while our computations are for dimension $d = 2$. The figure shows the bifurcation loci separating spectrally stable solitons (under the curve) from unstable ones (above the curve). The right panel shows a blowup of the left one close to the edge point of $p = 3$ and $b = 2$.

and dynamically unstable ones (over the curve) for fixed frequency $\omega = 1$. It is important to recall here that any pair $(b, \tilde{\omega} = 1)$ for a given b and fixed $\tilde{\omega}$ can be converted upon rescaling to a pair $(\tilde{b} = 1, \omega = 1/b^2)$, i.e., results pertaining to b variation for fixed $\tilde{\omega}$ are tantamount to ones with fixed \tilde{b} and variable ω . By using the latter representation, it is possible to connect to the well-known Vakhitov-Kolokolov criterion for the spectral stability, based on the monotonicity of the $P(\omega)$ dependence [27]. Increasing dependence of $P(\omega)$ (or, analogously, decreasing dependence of $P(b)$) is necessary for spectral stability, while a decreasing dependence (or increasing dependence of $P(b)$) leads to spectral (and dynamical) instability for the single-humped states considered herein. Furthermore, it should be noted that the limit of $b = 0$ is tantamount to $\omega \rightarrow \infty$, while $b \rightarrow 2$ corresponds to $\omega \rightarrow 1/4$ within the above scaling (the linear limit), setting the scales of variation of the respective parameters.

Representations of the dependence of P with respect to ω for different values of p can be found in Fig. 2. It can be clearly seen that in the case of $p = 3$, similarly to what happens for all values with $1 < p < 3$, P increases monotonically with ω , pertaining to a regime of spectral stability. Our numerical results seem to suggest the presence of a $p^* \approx 3.3$ (see once again the right end of the curves in the panels of Fig. 1). For $1 < p < p^*$, in line with Theorem 1, we find ground state minimizers for *all* values of $P \equiv \lambda$. By P here, we denote the squared L^2 norm due to its being tantamount to the optical power in the corresponding physical problem. For values of the exponent p that lie within $p^* < p < 5$, the power P features an interval of monotonic decrease with ω close to the linear limit (of dispersing waveforms). Indeed, the corresponding solutions near the linear limit are unstable, while for sufficiently large frequencies the solutions become spectrally stable, as seen in the top right panel which corresponds to $p = 5$. This finding also corroborates the results of Theorem 1, since in the latter interval, it is not possible to reach powers $P(\lambda)$ below the minimum of the corresponding curve. For $p > 5$ and below a critical, dimension-dependent threshold (which for our two-dimensional case is $p_{cr} = 6.565$), instabilities arise *both* for sufficiently small (near the linear limit) and sufficiently large (instabilities due to collapse) values of ω , as it is shown in the bottom left panel for $p = 6$; in this case, the only stable frequencies are the intermediate ones, corresponding to the interval of growing P . Finally, when going above the relevant critical value of p (see bottom right panel, corresponding to $p = 7$), the soliton is spectrally and dynamically unstable for *all* the frequencies, given the monotonically decreasing dependence of P with respect to ω . Notice that these findings for $p > 5 \equiv 1 + \frac{8}{d}$ complement in a natural way the rigorous results of Theorem 1.

Figure 3 showcases the relevant isotropic (radially symmetric) waveforms and a variety of different frequencies, starting from the highly nonlinear limit of large ω (where the width of the solution shrinks, while its amplitude grows), to progressively lower frequencies, eventually approaching the linear limit of small amplitude as $\omega \rightarrow 1/4$. It is important to note the logarithmic scale of the relevant colorbar, associated to continuously decreasing amplitudes as ω decreases. Noticeable also within this scale are the nodal lines of the solution, given the oscillatory nature of the linear tail as a result of the competition between the harmonic and biharmonic terms. Although this figure corresponds to $p = 3$, it is qualitatively similar to the outcome for other values of p .

We have made a similar analysis for the anisotropic case. The two-parameter diagram of p versus b is displayed in Fig. 4. Indeed, the phenomenology is quite similar to the isotropic case, although with some notable differences that can be observed not only near the right edge of the curve of Fig. 4 but also in the $P(\omega)$ plots for different values of p in Fig. 5. For

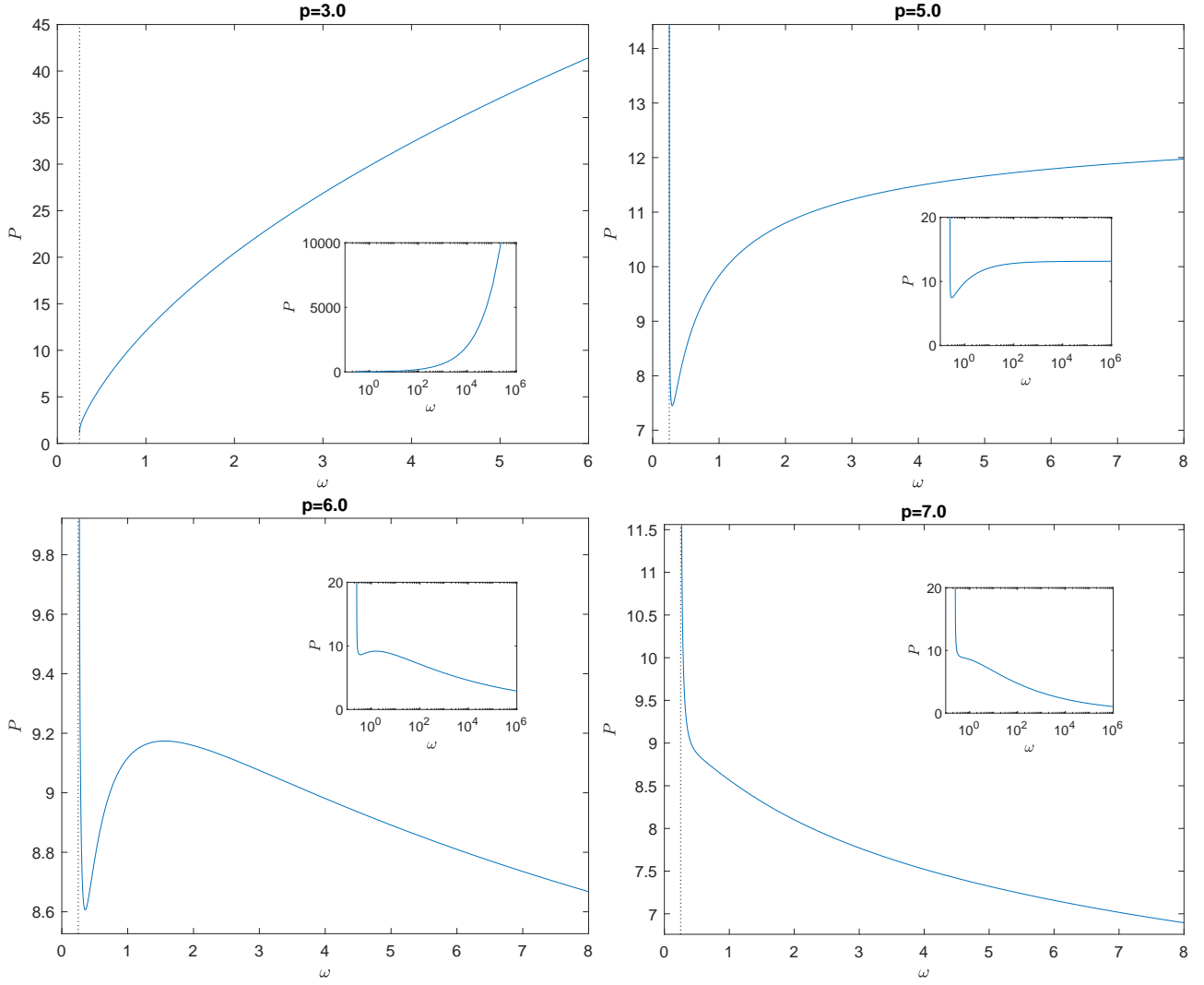


FIG. 2. Dependence of the squared L^2 norm, denoted by P , i.e., $P = \int_{\mathbf{R}^2} |u|^2$ for our computations, with respect to the frequency ω for different values of the nonlinearity exponent p , in the *isotropic* case for dimension $d = 2$. These plots showcase the different stability regimes that can be found herein (see text for more details). The insets show the same graph over an expanded interval of frequencies, using a semi-logarithmic scale for the latter.

low enough p (as, e.g., for $p = 2$), the soliton is stable for every frequency, and a solution exists for *all* values of $P \equiv \lambda$, in line with Theorem 2. However, contrary to the isotropic case, this monotonic dependence of P on ω does *not* persist up to $p = 3$. Indeed, there exists an interval of b 's (or, equivalently, of frequencies) for p roughly between 2.481 and 3 in our two-dimensional setting, whereby $P(\omega)$ presents a maximum and a minimum and, as a consequence, the soliton becomes unstable in that interval (as shown, e.g., in the plot for $p = 2.8$); this suggests that the linear limit is not approached in the same way as in the isotropic case near the critical point of $p = 3$. Incidentally, it is especially relevant to note that the linear limit itself bears nontrivial differences as now the second partial derivative only occurs along x direction. This leads, near the linear limit, to an oscillatory pattern *solely* along the x direction, while the solution becomes separable in the form $X(x) \times Y(y)$. This can be clearly observed in the relevant solution panels in Fig. 6.

It is also relevant to note here that our numerical results do not contradict Theorem 2, although in the very vicinity of the linear limit and for values of p between 2.5 and 3, we cannot fully confirm the relevant theory. In particular, a careful observation of Fig. 4, e.g., for $p = 2.8$ (top right panel) suggests a non-monotonic dependence of P on ω but as the linear limit is approached, we are unable to resolve the question of whether *all* values of P are accessible, as one approaches closer and closer to $\omega = 1/4$, in line with the expectations of Theorem 2. While the Theorem prompts us to expect that to be the case (and the numerics are also suggestive in this vein), the highly computationally expensive, anisotropic 2d computations needed have not allowed us to fully confirm this limit, which remains an interesting, open computational question for future studies.

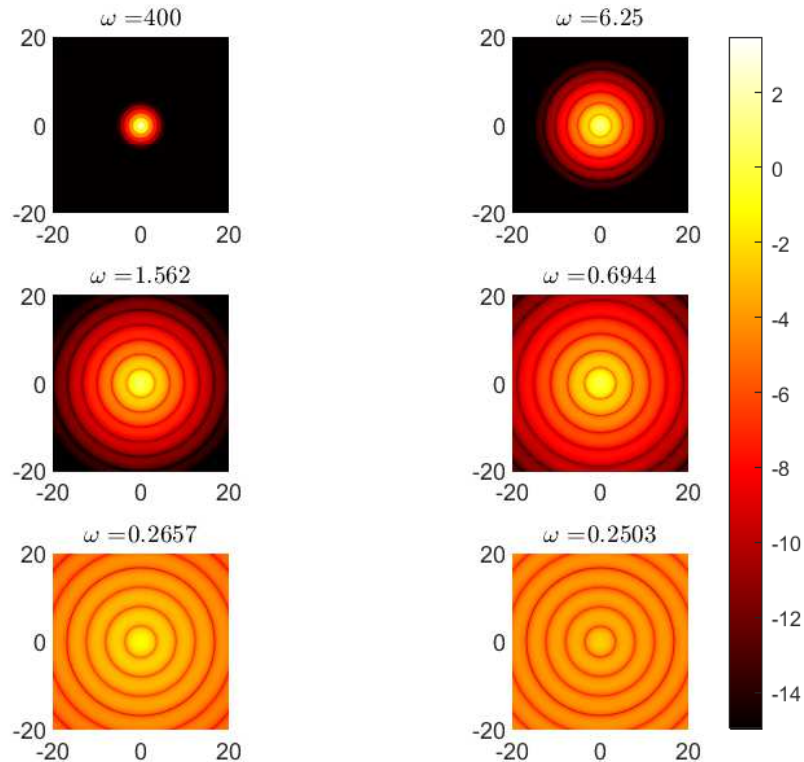


FIG. 3. Several examples of the waveform of the solitary waves with $p = 3$ in the isotropic case for different frequencies. We can observe how the solution profile changes from high ω to the linear limit of $\omega \rightarrow 0.25$. Notice the logarithmic scale of the colormap, and the (clear within that scale) zero-crossings of the solution. Figures for other values of p are qualitatively similar.

When p is increased from $p = 3$, we observe a similar phenomenology as in the isotropic case, i.e. the curve $P(\omega)$ is monotonically decreasing near the linear limit and becomes monotonically increasing (spectrally stable) after a local minimum (see the plot for $p = 5$). This phenomenology changes again (resembling the isotropic case) for $p > 5$, as shown in the plot for $p = 5.2$; here, an interval of stability for intermediate frequencies can be seen to arise. Finally, for sufficiently large values of p , again similarly to the isotropic limit, the waves become generically unstable for all frequencies, as illustrated by the monotonically decreasing dependence of $P(\omega)$ in the plot for $p = 6$. It is interesting to point out, however, that the relevant threshold is considerably lower in the anisotropic case where it is around $p = 5.407$ for $d = 2$, while in the isotropic one the threshold is around $p = 6.565$ for $d = 2$.

VI. CONCLUSIONS AND FUTURE CHALLENGES

In the present work, we have examined in a systematic way the properties of higher-dimensional NLS models with mixed dispersion with a numerical emphasis on the more computationally tractable case of $d = 2$. In particular, we have considered a setting in which there is a competition between a focusing quartic and a defocusing quadratic dispersion term. Our Theorems 1 and 2 have offered a rigorous perspective on the relevant phenomenology, providing bounds on the nonlinearity exponent (as a function of dimension) for which minimizers of the (squared) L^2 norm exist for all values of that quantity, as well as ones for which such minimizers do not exist for all powers. This has been done both for the isotropic case involving radial solutions, as well as for the anisotropic one where the second derivative term was only active along a particular direction. We have complemented these findings with detailed numerical results and corresponding multi-parameter diagrams detailing the stability of the single-humped states of the system. In both isotropic and anisotropic cases, we found that the exponent p of the nonlinear term is sufficiently small, the dependence of the power on the frequency is monotonic, while above a certain threshold more complex non-monotonic dependencies arise. Our numerical results for the case of $d = 2$ go beyond the accessible limits to our Theorems, identifying possible stable solutions even beyond the exponent bound of

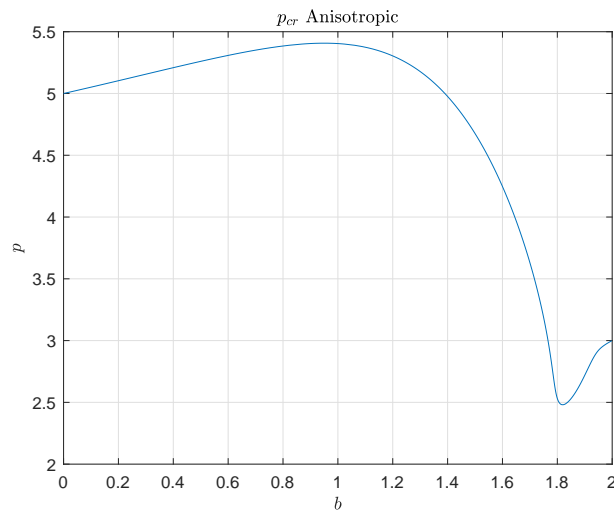


FIG. 4. Same as Fig. 1 but for the anisotropic case.

$p = 1 + 8/d$ (where d is the dimension), as well as identifying exponents beyond which no spectrally stable solutions arise.

While we believe that these results offer numerous insights into higher-dimensional systems with competing quadratic and quartic dispersions, there are also numerous open questions to consider. As concerns the problem examined herein, an important one concerns the close proximity of the linear limit for the anisotropic case when p is in the vicinity of $p = 3 \equiv 1 + 4/d$ (for our case of $d = 2$). More generally, for the case considered herein, it would be interesting to also examine if higher-excited states, including multi-soliton ones, as well as vortical ones are feasible and potentially also spectrally stable (and under what conditions). Additionally, numerical studies of the more computationally demanding case of $d = 3$ would also be worthwhile in connection to the Theorems presented herein. Last but not least, exploring similar questions with the recently accessible experimentally, even orders of dispersion [13] would also be of particular interest. Such studies are presently under consideration and will be reported in future publications.

ACKNOWLEDGMENT

A.S. acknowledges partial support from NSF-DMS # 1908626 and # 2204788. J.C.-M. acknowledges support from EU (FEDER program 2014-2020) through both Consejería de Economía, Conocimiento, Empresas y Universidad de la Junta de Andalucía (under the projects P18-RT-3480 and US-1380977), and MICINN and AEI (under the projects PID2019-110430GB-C21 and PID2020-112620GB-I00).

-
- [1] C. Sulem and P.L. Sulem, *The Nonlinear Schrödinger Equation*, Springer-Verlag (New York, 1999).
 - [2] M.J. Ablowitz, B. Prinari and A.D. Trubatch, *Discrete and Continuous Nonlinear Schrödinger Systems*, Cambridge University Press (Cambridge, 2004).
 - [3] M. J. Ablowitz, *Nonlinear Dispersive Waves: Asymptotic Analysis and Solitons*, Cambridge University Press (Cambridge, 2011).
 - [4] P. G. Kevrekidis, D. J. Frantzeskakis, and R. Carretero-González, *The defocusing nonlinear Schrödinger equation: from dark solitons and vortices to vortex rings*, SIAM (Philadelphia, 2015).
 - [5] A. Hasegawa, *Solitons in Optical Communications*, Clarendon Press (Oxford, NY 1995).
 - [6] Yu.S. Kivshar and G.P. Agrawal, *Optical solitons: from fibers to photonic crystals*, Academic Press (San Diego, 2003).
 - [7] L.P. Pitaevskii and S. Stringari, *Bose-Einstein Condensation*, Oxford University Press (Oxford, 2003).
 - [8] C.J. Pethick and H. Smith, *Bose-Einstein condensation in dilute gases*, Cambridge University Press (Cambridge, 2002).
 - [9] M. Kono and M. M. Skorić, *Nonlinear Physics of Plasmas*, Springer-Verlag (Heidelberg, 2010).
 - [10] E. Infeld and G. Rowlands, *Nonlinear Waves, Solitons and Chaos*, Cambridge University Press (Cambridge, 1990).
 - [11] A. Blanco-Redondo, C. Martijn de Sterke, J.E. Sipe, T.F. Krauss, B.J. Eggleton, and C. Husko, *Nature Communications*, **7**, 10427 (2016).
 - [12] A.F.J. Runge, D.D. Hudson, K.K.K. Tam, C.M. de Sterke, A. Blanco-Redondo, *Nature Photonics* **14**, 492 (2020).
 - [13] A.F.J. Runge, Y.L. Qiang, T.J. Alexander, M.Z. Rafat, D.D. Hudson, A. Blanco-Redondo, and C.M. de Sterke, *Phys. Rev. Research* **3**, 013166 (2021).
 - [14] A. Demirkaya and M. Stanislavova, *DCDS-B* **24**, 197 (2019).

- [15] R. Decker, A. Demirkaya, P.G. Kevrekidis, D. Iglesias, J. Severino, and Y. Shavit, *Commun. Nonlinear Sci. Numer. Simulat.*, **97**, 105747 (2021).
- [16] I. Posukhovskiy and A. Stefanov, *DCDS-A* **40**, 4131 (2020).
- [17] K.K.K. Tam, T.J. Alexander, A. Blanco-Redondo, and C.M. de Sterke, *Phys. Rev. A* **101**, 043822 (2020).
- [18] V.I. Karpman, *Phys. Lett. A* **193**, 355 (1994).
- [19] V.I. Karpman, *Phys. Rev. E* **53**, R1336 (1996).
- [20] J. Yang (ed.), *Nonlinear waves in integrable and nonintegrable systems*, SIAM (Philadelphia, 2010).
- [21] D.-S. Wang, W. Han, Y. Shi, Z. Li, and W.-M. Liu, *Commun. Nonlinear Sci. Numer. Simul.* **36**, 45 (2016).
- [22] R. Gong, Y. Shi, D.-S. Wang, *DCDS* (2022), <http://dx.doi.org/10.3934/dcds.2022018>
- [23] G.A. Tsolias, R.J. Decker, A. Demirkaya, T.J. Alexander, and P.G. Kevrekidis, *J. Phys. A: Math. Theor.* **54**, 225701 (2021).
- [24] T. Kato, *Perturbation theory for linear operators*, Springer-Verlag (Berlin, 1995).
- [25] L. Grafakos, *Classical and modern Fourier analysis*, Pearson (London, 2004).
- [26] P.L. Lions, *Ann. Inst. Henri Poincaré (C) Anal. Non Linéaire* **1**, 109 (1984).
- [27] T. Kapitula and K. Promislow, *Spectral and dynamical stability of nonlinear waves*, Springer-Verlag (New York, 2013).

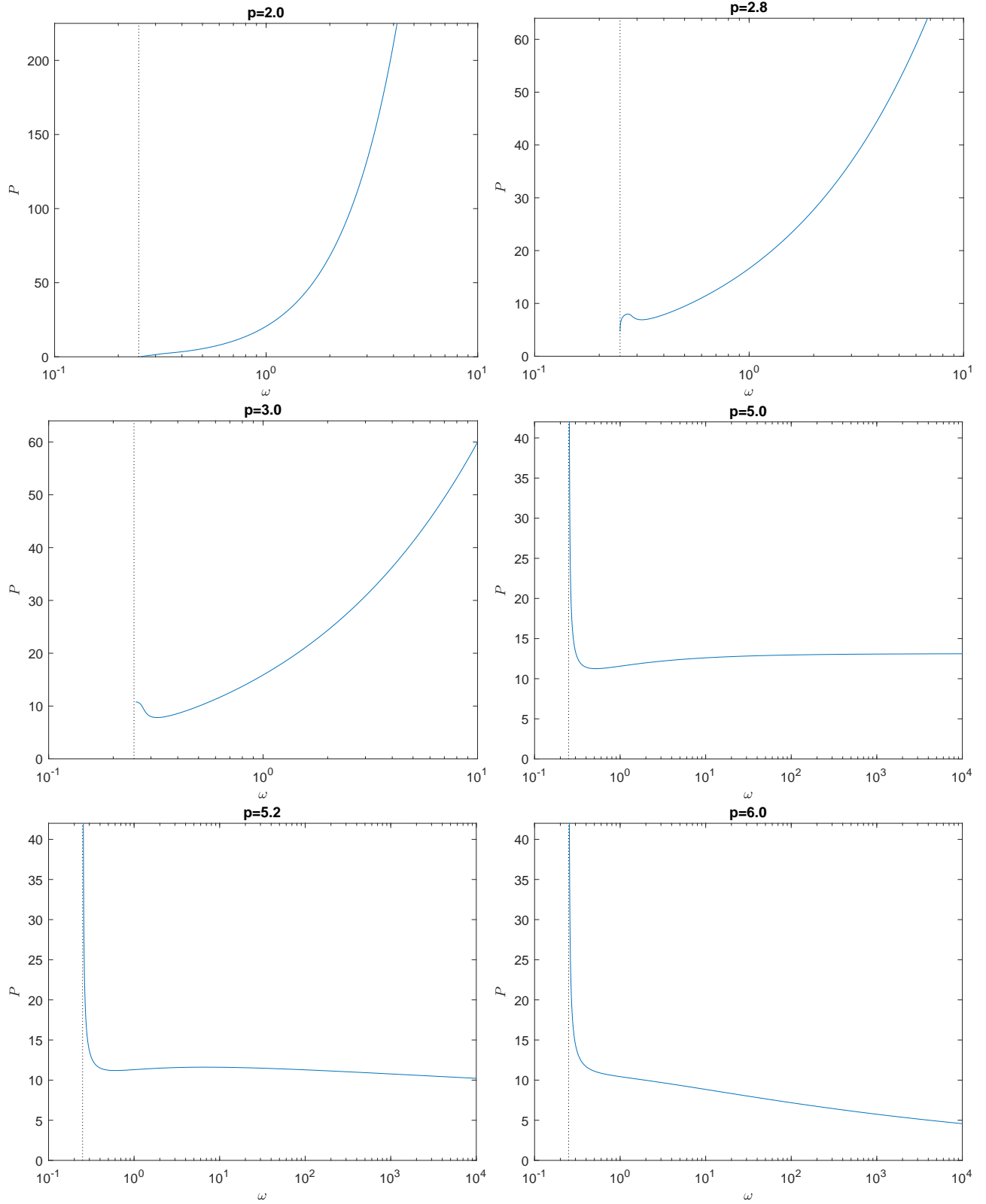


FIG. 5. Same as Fig. 2 but for the anisotropic case and for different values of p . Again, a semi-logarithmic scale has been used for the frequencies.

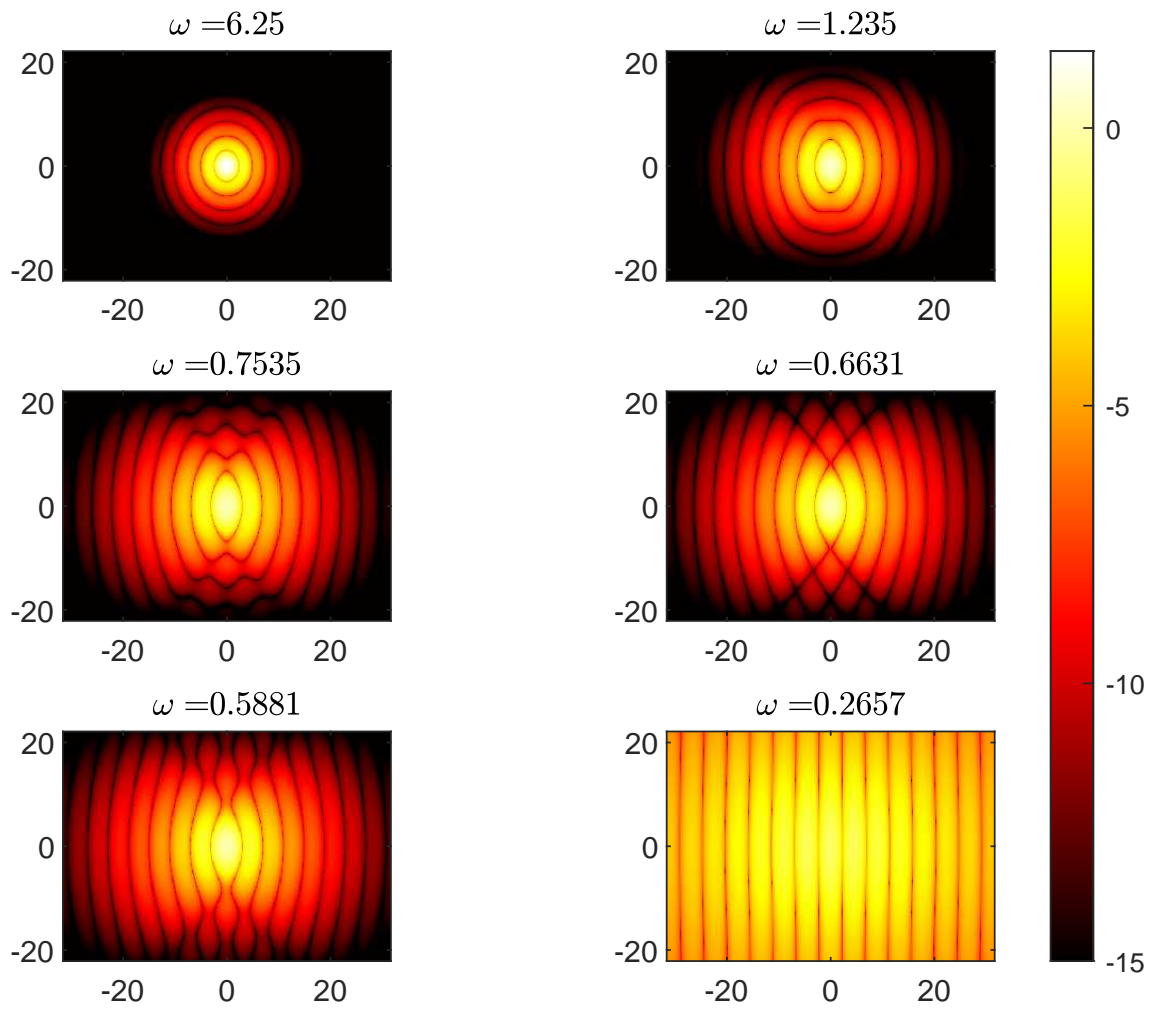


FIG. 6. Same as Fig. 3 but for the anisotropic case with $b = 1$. Contrary to the isotropic case, the anisotropy reflects in the solution as it acquires, when approaching the linear limit $\omega \rightarrow 0.25$ a separable form in the x and y dependence with the nodal lines being uniform along direction y .